Non-ergodic site response model based on local recordings for Menta Dam site

A. Vecchietti
*Department of Civil and Mechanical Engineering at University of Cassino and Southern Lazio, Cassino &
Department of Engineering at University of Perugia, Perugia, Italy*

J. P. Stewart
Department of Civil and Environmental Engineering at University of California Los Angeles, Los Angeles, California

M. Cecconi & V. Pane
Department of Engineering at University of Perugia, Perugia, Italy

G. Russo
*Department of Civil and Mechanical Engineering at University of Cassino and Southern Lazio, Cassino, &
Department of Earth Science, Environment and Resources at University of Napoli Federico II, Napoli, Italy*

ABSTRACT: The paper describes the development of a non-ergodic site response model for a strategic site in the Aspromonte mountains, in Southern Italy. Fractured metamorphic rocks belonging to Calabrian complex outcrop in this area, located in a region where Southern Apennines crustal faults and subduction of the Calabrian Arc contribute to the seismic hazard. At the site, three accelerometers are installed since 2016 as part of the monitoring system of the Menta Dam, a bituminous-faced rockfill dam constructed for the water supply of the region. Ground motions recorded at the site and elsewhere from regional crustal and subduction earthquakes have been used to evaluate region-specific source and path adjustment to global ground motion models (GMMs). Those regionally adjusted GMMs have, in turn, been used to evaluate the mean bias of site-specific recordings, which is used to estimate non-ergodic site response for the dam site. This analysis highlights that site-specific site response is appreciably larger than the global average prediction of GMMs for periods lower than 0.4s. A non-ergodic GMM is developed that accounts for these effects to be used in subsequent Probabilistic Site Hazard Analysis (PSHA).

1 INTRODUCTION

Menta dam is a bituminous-faced rockfill dam that impounds a 18 million m^3 reservoir for water supply of Calabria region, in Southern Italy. The dam is located in the Aspromonte National Park, in the southern section of the Apennines, at an altitude of about 1400m a.s.l.. Complex seismogenic processes are taking place in the region, and geodynamics and tectonic framework interpretation have been the subject of lively debate over the last 30 years (Carafa et al. 2018, Tiberti et al. 2017, Galli & Peronace, 2015, Presti et al. 2013, Monaco & Tortorici 2000, Valensise & Pantosti 1992 and references herein). In addition, earthquakes occurred in Calabria are among the strongest in Italy's seismic history (see DISS Database, http://diss.rm.ingv.it/diss/).

A hydraulic and seismic safety analysis of Menta dam has been recently completed (Vecchietti et al. 2018). As part of this assessment, a probabilistic seismic hazard analysis (PSHA) has been carried out, with particular attention being paid to site-specific site response effects. In a classical PSHA, the seismogenic sources are combined with appropriate ground motion models (and associated uncertainties) for predicting seismic intensity measures and, for a fixed probability, uniform hazard spectra. In this study, the recordings of earthquakes measured by accelerometers installed at the dam site have been analyzed, along with recordings available for those same events at other stations in the region, to develop regionally-adjusted ground motion models and a non-ergodic site term for the location of interest.

In the following, the procedure used for developing regional correction of Ground Motion Models is described. Following procedures given in Stewart et al. (2017), the Menta dam non-ergodic site response term is then derived. The results are compared to those obtained with ergodic models.

2   REGIONAL GROUND MOTION MODELS

Ground Motion Models (GMMs) are semi-empirical relations that allow estimation of seismic intensity measures (e.g. PSA, PGA, PSV) given a set of predictors related to characteristics of the event (e.g. magnitude, focal mechanism) and site (location and site parameters). These models were developed from empirical regressions of observed amplitudes in available databases of recordings; these equations are applied in similar seismogenic contexts following the assumption that average source, path, and site effects from global databases may apply for any site (ergodicity). Typically, a GMM gives the mean of an intensity measure in log units $(\mu_{lnZ})_{ij}$ for an event i, at site j, as a function of additive source terms $(F_{E,i})$, path terms $(F_{P,i})$ and site terms $(F_{S,i})$, respectively:

$$\left(\mu_{lnZ}\right)_{ij} = F_{E,i} + F_{P,ij} + F_{S,ij} \tag{1}$$

as well as its standard deviation (σ).

Site-specific response will generally differ from the global average prediction given by the GMMs due to local conditions. For the present application, source and path terms in two global GMMs, namely BSSA14 (Boore et. al 2014) for crustal earthquakes and BCHydro16 (Abrahamson et al. 2016) for subduction earthquakes are examined for use in the Southern Calabria region by validating model prediction with regional recordings, including dam site recordings.

2.1   *Regional seismicity and recordings dataset*

The Calabrian Arc is a portion of the complex plate boundary between the Eurasian and African plates (Figure 1a). The plate converging boundary results in the subduction of Ionian oceanic crust beneath the southern margin of the European plate, still ongoing beneath the Calabria region. The thrust structure of the accretionary wedge spans into the Ionian Sea for about 300 km (Polonia et al. 2016). In this framework, large normal faults have developed on the Tyrrhenian side of the upper plate, parallel to the Arc, on top of the subduction interface. In addition to normal faults, strike-slip faults dissect the extensional axis of the Calabrian Arc. Over the past five centuries Southern Calabria was struck by several crustal **M** 6+ earthquakes, including the seismic sequence of February-March 1783 (from Gioia Tauro Plain toward south Catanzaro, max Mw 7.0), the 16 November 1894 event (northern end of the Messina Straits, Mw 6.1), the 8 September 1905 earthquake in the Gulf of Sant'Eufemia (Mw 7.0) and the 28 December 1908 earthquake in the Messina Straits (Mw 7.1). Below this accretionary wedge, there are no records of large seismic events along the shallow portion of the plate interface, while present-day deep seismicity data provide evidence of in-slab events down to a depth of more than 400 km (Chiarabba et al. 2005).

Twenty events have occurred in the region between October 2016 and February 2018, which are considered in the present study. Records span from **M** 3.3-5.8 and are located within a distance range 6 km < R_{epi} < 350 km from the site of Menta dam. These events originate from both crustal faults and deep in-slab subduction seismicity; they have been recorded by accelerometers installed on the two abutments and along the southern slope of the reservoir. Recordings of the same events have been retrieved from Italian Accelerometric Network data managed by DPC (RAN-DPC) to build a database of 232 recordings for this work. For each event-station couple, epicentral distance, R_{epi}, closest distance to the ground surface-fault projection, R_{JB}, and hypocentral distance, R_{hypo}, were computed. Each station has also been characterized with assigned $V_{S,30}$ values: for those locations without velocity measurements, correlation with lithology adopted by Scasserra et al. (2009) has been used. Figure 1 b-c shows the location of the events and magnitude – distance features of the dataset.

All the raw recordings have been processed to remove high-frequency noise and late-triggered records in the time series (acceleration *vs.* time). The processing procedure is consistent with Boore & Bommer (2005) and the PEER record processing procedure (Ancheta et al. 2014). In pre-processing, instrumental response and the raw record mean are removed, applying - where appropriate - a *cosine taper* to cut unnecessary signal. We applied a low- and high-pass acausal Butterworth filters in the frequency domain, selecting corner frequencies by visual examination
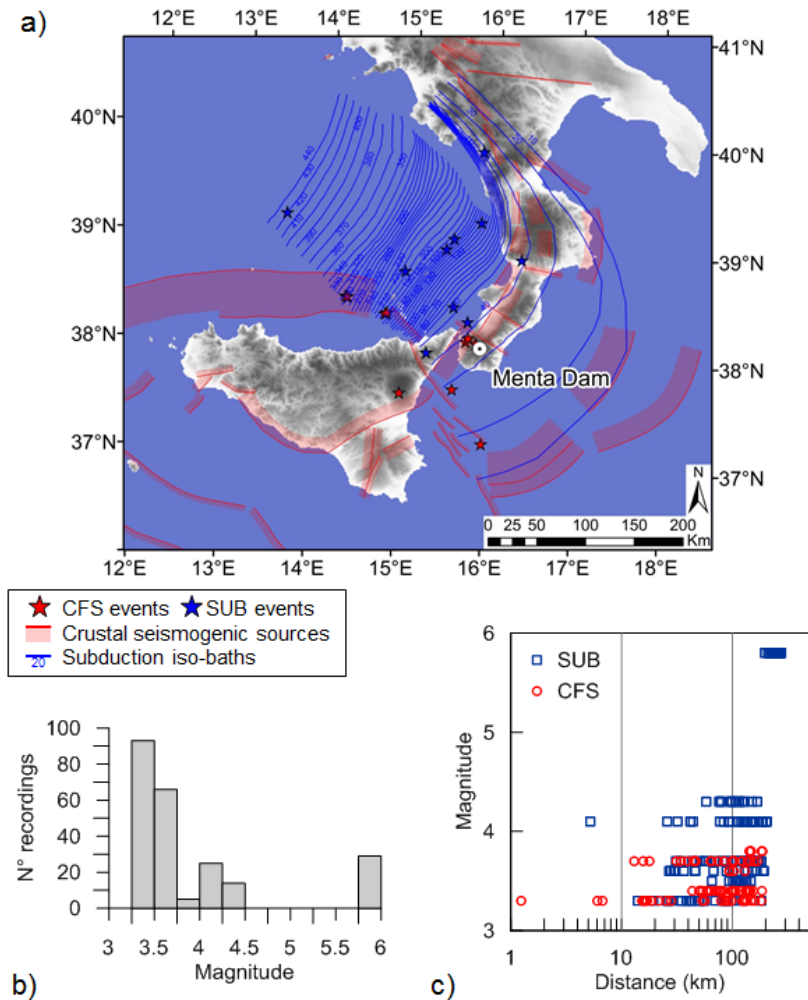
Figure 1. a) Sketch map that illustrates the main tectonic features of the study area (from DISS database, DISS Working group 2018) and the n.20 events considered for the present study; b) and c) characteristics of the recording database in terms of magnitude and distance. CFS: crustal fault source, SUB: subduction.

of the Fourier amplitude spectra and integrated displacements. If necessary, a simple baseline correction was applied for cases where filtering did not remove non-physical trends in the displacement time series. Finally, each pair of horizontal orthogonal component time series has been combined with the algorithm by Wang et al. (2018) in order to compute the median rotated azimuth-independent Pseudo-Spectral Acceleration spectrum (RotD50, Boore 2010) for the usable band of each record.

2.2 *Analysis of residuals*

Residuals analyses are performed to compare the predictions of available ground motion models to regional and site-specific recordings. Two models have been used for representing active crustal fault and subduction-in slab events respectively:

- Boore at al. (2014) BSSA14 model, which is based on NGA-West2 database records (Ancheta et al., 2014) and valid for active crustal regions. It has a regional correction term for Italy;
- Abrahamson et al. (2016) BCHydro16 model, which is the most recent model for subduction earthquakes with **M** > 5. This model was extended for consideration of **M** ≤ 5 events in the present work.

The applicability of the two models in the Calabria region has been evaluated using residuals analysis. The total residual (R_{ij}) is defined as:

$$R_{ij} = \ln z_{ij} - (\mu_{\ln Z})_{ij} \tag{2}$$

where z_{ij}, is the observation of event i at station j and $(\mu_{\ln Z})_{ij}$ is model prediction. The total residuals can be decomposed into (Al Atik et al. 2010):

$$R_{ij} = \eta_{Ei} + \delta W_{ij} \tag{3}$$

where η_{Ei} is the between-events residual, i.e. the event-term (approximately the average misfit of recordings of an earthquake (E) relative to the median GMM), and δW_{ij} is the within-event residual, corresponding to the difference between the total residual and η_{Ei}. Within-event residuals can be non-zero due to errors in the path or site models used in the GMMs. If the path model is not regionally biased, the contribution of path errors to within-event residuals computed from multiple regional events should average to zero, leaving site-related errors as the remaining potential source of bias. These site-related biases for each station are referred to as the station site-term, η_{Sj} (defined as the average δW_{ij} recorded at station j). The quantity ε_{ij} is the remaining residual after site- and event-terms are subtracted from total residuals:

$$\delta W_{ij} = \eta_{Sj} + \varepsilon_{ij} \tag{4}$$

The quantities η_{Ei} and η_{Sj} are zero mean random variables and their standard deviation, τ and ϕ_{S2S}, quantify the variability of ground motions between events and sites. The total single-station standard deviation σ_{SS} omits the between site variability, and can be computed as (Rodriguez-Marek et al. 2011):

$$\sigma_{SS} = \sqrt{\tau^2 + \phi_{SS}{}^2} \quad \text{and} \quad \phi_{SS} = \sqrt{\frac{\sum_j \sum_{i=1}^{NE_j} \varepsilon_{ij}{}^2}{\sum_j NE_j - 1}} \tag{5}$$

The quantity ϕ_{SS} is the event-corrected single-station standard deviation and NE_j is the total number of events recorded at station j.

  PSA residuals derived from the original GMMs demonstrate local biases. Although not shown here for brevity, the observed biases are two-fold: (1) for crustal earthquakes, the within-event residuals drift with respect to distance, indicating bias in the path term, and (2) for subduction-in slab earthquakes, between-event residuals drift with magnitude, indicating bias in the source term. In particular, for crustal earthquakes, observations indicated that distance attenuation was faster than model prevision and, conversely, that for extending BCHydro16 Model to **M** < 5 regional data, a slower magnitude-scaling was needed. Accordingly, we modified the GMMs for regional conditions by adjusting the path function for the BSSA14 model (F_P) and the magnitude-scaling term for BCHydro16 model (F_M): the constant terms c_1 and θ_4 were revised introducing modifications Δc_1 and $\Delta\theta_4$, as follows:

$$F_P = \left[c_1 + \Delta c_1 + c_2 (M - M_{ref}) \right] \cdot \ln\frac{R}{R_{ref}} + (c_3 + \Delta c_3) \cdot (R - R_{ref}) \tag{6a}$$

$$F_M = (\theta_4 + \Delta\theta_4) \cdot [M - 7.8] + \theta_{13} \cdot (10 - M)^2 \tag{6b}$$

In Eq.(6), R is a function of distance R_{JB}, M represents magnitude, and c_2, c_3, Δc_3, M_{ref}, R_{ref}, θ_{13} are other constant terms. Figure 2 shows that this modification of the constant terms (Δc_1 and $\Delta\theta_4$) was statistically significant, which is indicated by zero being outside the 95% confidence interval of the adjustment at most periods. Residuals were then re-computed and partitioned as described here. Figure 3 shows the resulting within-event residuals δW_{ij}, which shows that the regionally-adjusted models perform well. Moreover, standard deviations of the residual components (between-event τ, and site-corrected term ϕ_{SS} in Figure 4) are consistent with other studies performed in Italy (Luzi et al. 2014, Lanzano et al. 2017) and do not show a significant trend with magnitude (homoscedasticity).
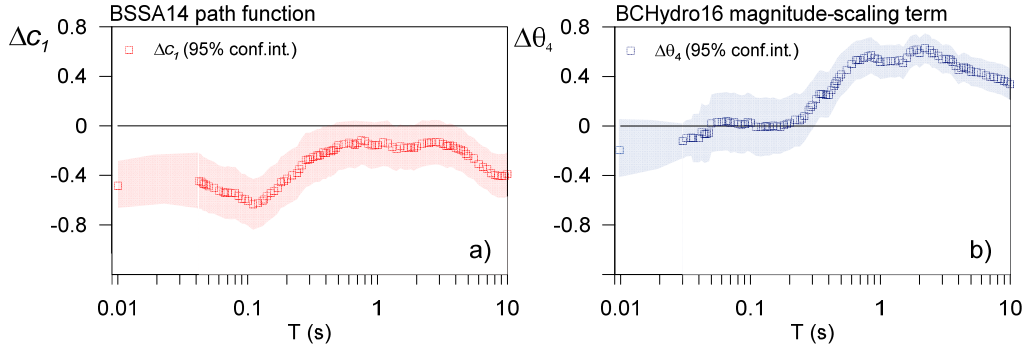
Figure 2. a) Adjustments to path function (F_P) for the BSSA14 model, showing the reduction of constant term, Δc_1. b) Adjustments to magnitude-scaling term (F_M) for BCHydro16 model, showing the increase of constant term, $\Delta\theta_4$. Note that, per Eq. 6b and for M < 7.8, increasing θ_4 implies a reduction of F_M.
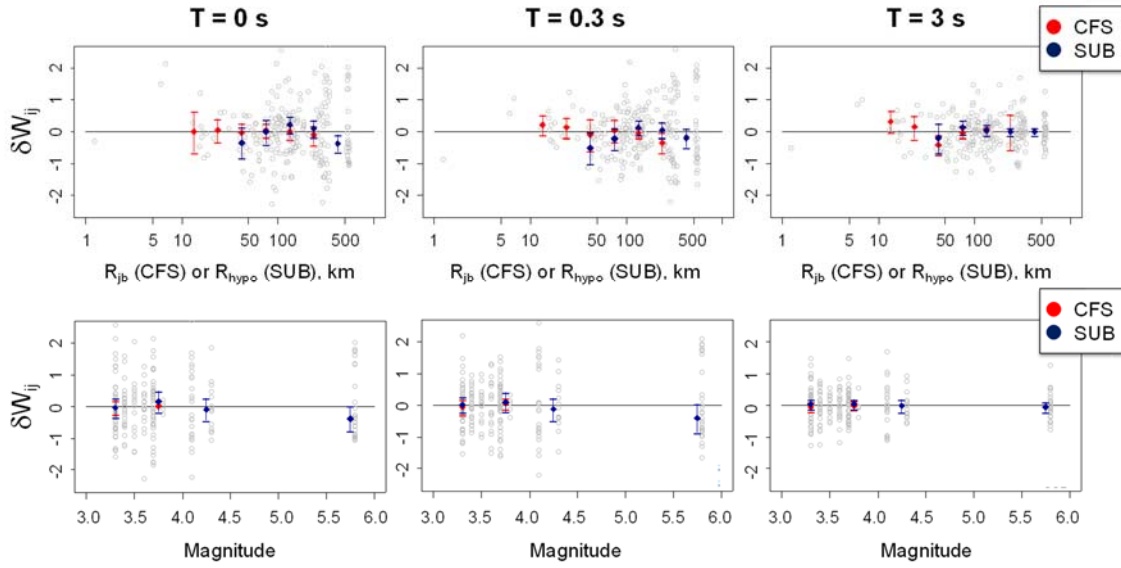

Figure 3. Event- and site-corrected residuals δW_{ij} as function of Distance (R_{JB} or R_{hypo} for crustal and subduction seismic recordings) and Magnitude for example periods T= 0 (PGA), 0.3s, 3s for the regional-adjusted models. The dot symbols represent the mean and the bars represent ±95% confidence level for binned data. CFS: crustal fault source, SUB: subduction.
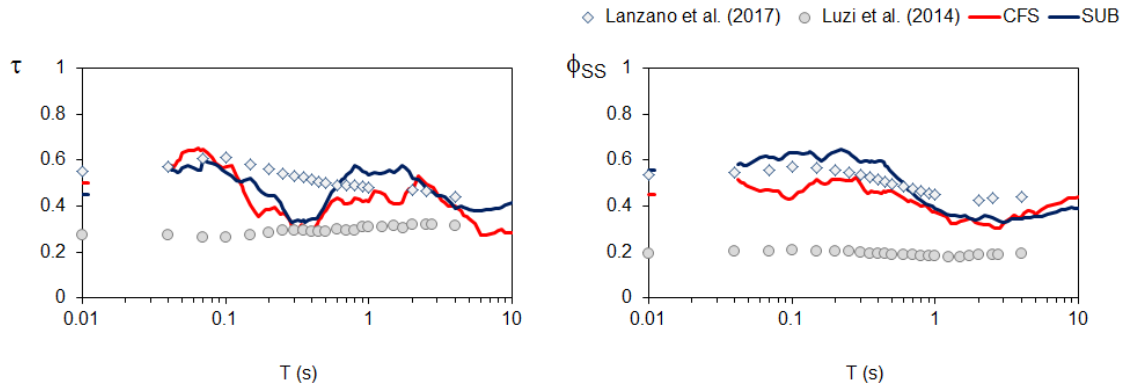

Figure 4. Between-event (τ) and site-corrected (ϕ_{SS}, i.e. single-station sigma) standard deviation as a function of period T for the regional-adjusted models for crustal fault (CFS) and subduction (SUB) earthquakes, compared to studies of single-station sigma for Italian stations by Luzi et al. (2014) and Lanzano et al. (2017).

3 SITE AMPLIFICATION FROM THE RECORDINGS

The regionally-adjusted GMMs were used for evaluating non-ergodic site response at Menta Dam site. Following Stewart et al. (2017), site mean amplification is represented by the bias of on-site recordings from regional GMMs. Specifically, the linear site response estimate is the sum of the site term η_{Sj} at the Menta Dam site and the ergodic site term for the site's $V_{S,30}$ given by the GMMs:

$$F_{S,ij} = F_{S,i}\left(V_{S,30,j}\right) + \eta_{Sj} \tag{7}$$

The calculation in Eq.(7) uses the ergodic site term F_S, which depends on $V_{S,30}$. Unfortunately, in-situ measurements of V_S are not available for the metamorphic rocks that outcrop at the site. The site geology consists of micascists and paragneiss, and the shallower rock mass is characterized by a marked grade of alteration and relevant fracture systems. Values of Rock Quality Designation (RQD) are between 35% and 70% in the upper 10 m, and generally larger than 70% at large depths, based on borehole samples dated to 1977-79. V_S has been then inferred from laboratory tests on rock samples and the distribution of RQD index with depth, and the calculated value of $V_{S,30}$ for the profile is 1000m/s. While Eq.(7) describes linear amplification, nonlinear effects are not expected to be significant given the stiffness of the rock. As shown in Figure 5, site response is larger than the global average prediction of GMMs for period T < 0.4s. The patterns are similar for both event types. While the magnitude of the site response is larger in the subduction case, there is no physical explanation for why these should differ, and the differences are of marginal statistical significance. As a result, the site response model adopted for analysis is based on the average within-event residual for both event types.

4 DISCUSSION

Spectra provided by regional models with ergodic and non-ergodic site response (the latter being specific to the Menta dam site) are compared to those from global models (BSSA14 and BCHydro16) with ergodic site response in Figure 6. These plots show the impact of regional-adjustments and site-specific site term on predicted ground motions. Spectra are computed for event/distance combinations representative of controlling sources. For crustal sources, these are $\mathbf{M} = 5, 6$ and $R_{JB} = 10, 30, 100$ km, and for subduction-in slab sources these are $\mathbf{M} = 6,7$ and $R_{hypo} = 32, 64, 112$ km. All results apply for $V_{S,30} = 1000$m/s. Two factors cause the regional crustal model predictions to be lower than the global model – faster distance attenuation and a negative (downward) adjustment of the constant term. Similarly, for subduction sources flatter magnitude scaling and a lower constant term cause modest reductions to spectra. An appreciable fraction of the adjustment is from the constant term, which is admittedly uncertain, especially given the small magnitude of the crustal events used in the analysis. Data from such events can produce misleading results, especially for short period oscillator responses (Stafford et al. 2017). As a result, application of the model with these reductions in the constant term may not be advisable. The site-specific site response partially offsets these reductions of the regional models relative the global models at short periods (< ~0.3 sec). The peak in the site response near 0.08 sec suggests a possible resonance effect that is not captured by the ergodic model. We are unable to confirm the cause of this effect due to lack of a suitable V_S profile.

5 CONCLUSIONS

Regional ground motion models have been developed by adjusting certain components of global ground motion models based on analysis of local recordings in the Calabria region. One of the more significant adjustments is to the constant term, which is uncertain when estimated from small magnitude data, as in the case here. Seismic site response at the Menta dam site in Calabria has been evaluated based on interpretation of on-site recordings. The non-ergodic site term at the Menta dam site has been developed for subsequent use in Probabilistic Seismic Hazard Analysis (PSHA). Site-specific uniform hazard spectra will be obtained combining these Ground Motion Models with a source model which includes all the relevant seismic sources for the area. It is necessary to consider epistemic uncertainties in the model adjustments in these hazard analyses.
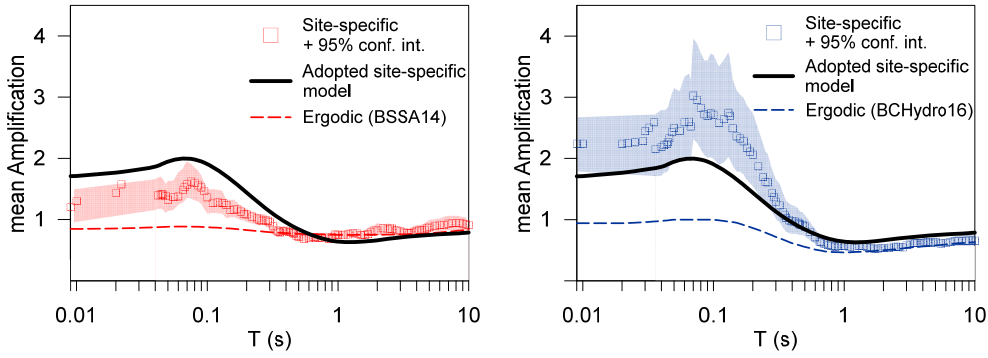
Figure 5. BSSA14 and BCHydro16 regional-adjusted model prediction (ergodic) relative to site-specific (non-ergodic) linear site amplification term of the GMMs to be used in site-specific PSHA. Red plot: crustal fault source (CFS), blue plot: subduction (SUB).
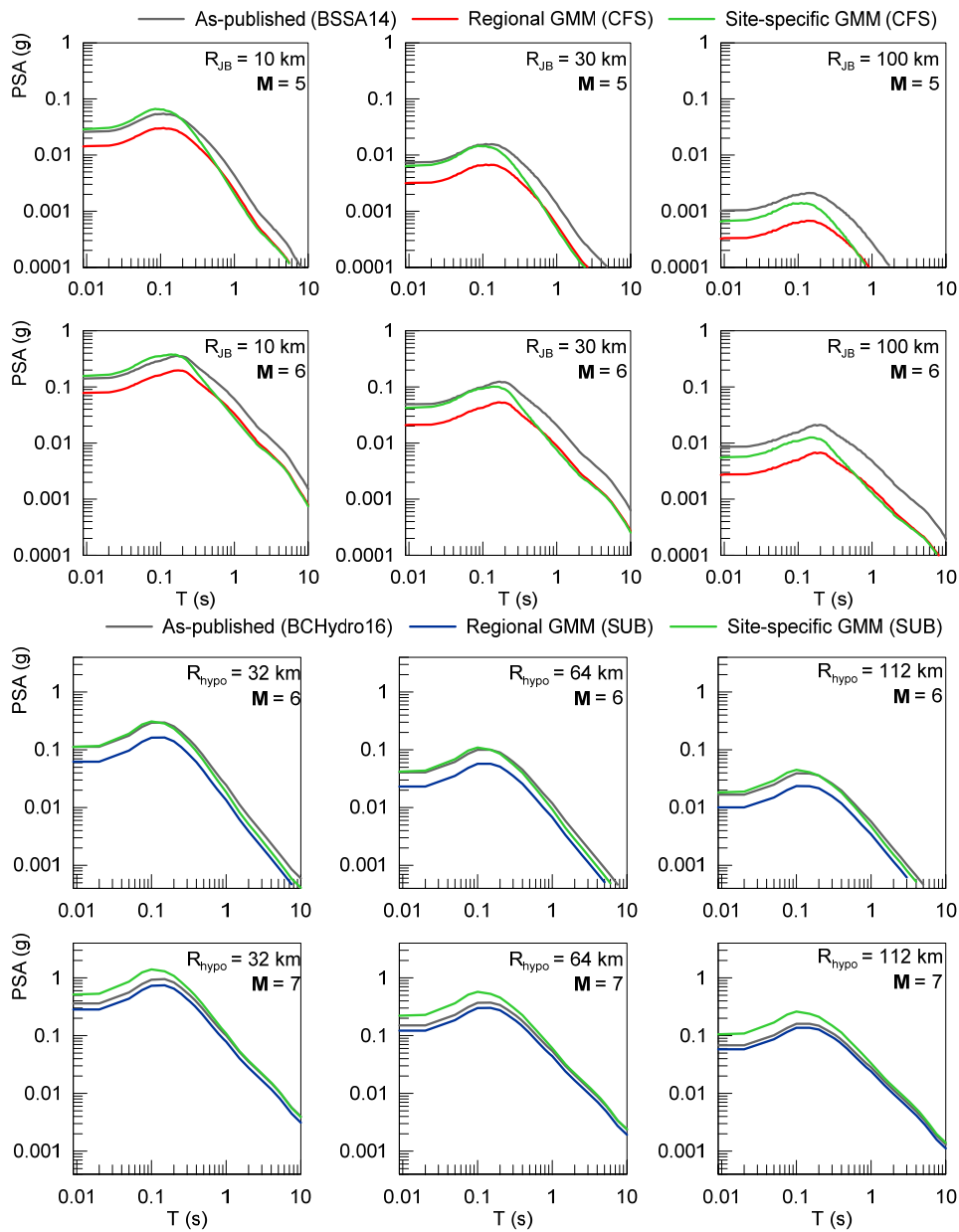

Figure 6. Prediction of regional and site-specific models, compared to as-published models.

REFERENCES

Abrahamson, N., Gregor, N. & Addo, K. 2016. BC Hydro ground motion prediction equations for subduction earthquakes. *Earthquake Spectra* 32(1): 23–44.

Al Atik, L., Abrahamson, N.A., Bommer, J.J., Scherbaum, F., Cotton, F. & Kuehn, N. 2010. The variability of ground motion prediction models and its components. *Seism. Research Letters* 81: 794–801.

Ancheta, T.D., Darragh, R.B., Stewart, J.P., Seyhan, E., Silva, W.J., Chiou, B.S.J., Wooddell, K.E., Graves, R.W., Kottke, A.R., Boore, D.M., Kishida, T. &Donahue, J.L. 2014. NGA-West2 database. *Earthquake Spectra* 30:989–1005.

Boore D.M 2010. Orientation-independent, nongeometric-mean measures of seismic intensity from two horizontal components of motion. *Bulletin of the Seismological Society of America* 100(4): 1830–1835.

Boore D.M. & Bommer J.J. 2005. Processing of strong-motion accelerograms: needs, options and consequences. *Soil Dynamica and Earthquake. Engineering* 25:93–115.

Boore, D.M., Stewart J.P., Seyhan, E. & Atkinson, G.M. 2014. NGA-West 2 equations for predicting PGA, PGV, and 5%-damped PSA for shallow crustal earthquakes. *Earthquake Spectra* 30:1057–1085.

Carafa, M.M.C., Kastelic, V., Bird, P., Maesano, F.E. & Valensise, G. 2018. A geodetic gap in the Calabrian Arc: Evidence for a locked subduction megathrust?. *Geophysical Research Letters* 45:1794–1804.

Chiarabba, C., Jovane, L. & Di Stefano, R. 2005. A new view of Italian seismicity using 20 years of instrumental recordings. *Tectonophysics* 395: 251-268

DISS Working Group. 2018. Database of Individual Seismogenic Sources (DISS), Version 3.2.1: A compilation of potential sources for earthquakes larger than M 5.5 in Italy and surrounding areas.

Galli, P.A.C. & Peronace, E. 2015. Low slip rates and multimillennial return times for Mw 7 earthquake faults in southern Calabria (Italy). *Geophysical Research Letters* 42: 5258-5265.

Lanzano, G., D'Amico, M., Felicetta, C., Luzi, L. & Puglia, R. 2017. Update of the single-station sigma analysis for the Italian strong-motion stations. *Bulletin of Earthquake Engineering* 15(6): 2411-2428.

Luzi, L., Bindi, D., Puglia, R., Pacor, F. & Oth, A. 2014. Single-station sigma for Italian strong-motion stations". *Bulletin of Seismologic Society of America* 104: 467–483.

Monaco, C. & Tortorici, L. 2000. Active faulting in the Calabrian arc and eastern Sicily. *Journal of Geodynamics* 29:407-424.

Polonia, A., Torelli, L., Artoni, A., Carlini, M., Faccenna, C., Ferranti, L., Gasperini, L., Govers, R., Klaeschen, D., Monaco, C., Neri, G., Nijholt, N., Orecchio, B. & Wortel, R. 2016. The Ionian and Alfeo-Etna fault zones:new segments of an evolving plate boundary in the central mediterranean sea?. *Tectonophysics 675:69-90*

Presti, D., Billi, A., Orecchio, B., & Totaro, C. 2013. Earthquake focal mechanisms, seismogenic stress, and seismotectonics of the Calabrian Arc, Italy. *Tectonophysics* 602: 153–175.

RAN-DPC. Rete Accelerometrica Nazionale. Dipartimento della Protezione Civile - Presidenza del Consiglio dei Ministri. http://www.protezionecivile.gov.it/jcms/it/ran.wp .

Rodriguez-Marek, A., Montalva, G.A, Cotton, F. & Bonilla F. 2011. Analysis of Single-Station Standard Deviation Using the KiK-net Data. *Bulletin of Seismologic Society of America* 101(3): 1242–1258.

Scasserra, G., Stewart, J.P., Bazzurro, P., Lanzo, G. & Mollaioli, F. 2009. A comparison of NGA ground motion prediction equations to Italian data. *Bulletin of Seismologic Society of America* 99:2961–2978.

Stafford, P.J., Rodriguez-Marek, A., Edwards, B., Kruiver, P.P., Bommer, J.J., 2017. Scenario Dependence of Linear Site-Effect Factors for Short-Period Response Spectral Ordinates, *Bulletin of Seismologic Society of America* 107(6): 2859–2872.

Stewart, J.P., Afshari, K. & Goulet, C. 2017. Non-Ergodic Site Response in Seismic Hazard Analysis. *Earthquake Spectra* 33(4): 1385–1414.

Tiberti, M.M., Vannoli, P., Fracassi, U., Burrato, P., Kastelic, V. & Valensise G. 2017. Understanding seismogenic processes in the Southern Calabrian Arc: a geodynamic perspective. *Italian Journal of Geosciences* 136(3): 365-388.

Valensise, G. & Pantosti, D. 1992. A 125 kyr-long geological record of seismic source repeatability: the Messina Straits (southern Italy) and the 1908 earthquake (Ms 7/2). *Terra Nova* 4: 472-483.

Vecchietti, A., Russo, G., Cecconi, M. & Pane, V. 2018. Seismic performance of a bituminous-faced rockfill dam. *Proc. 16th European Conference of Earthquake Engineering, Thessaloniki, 18 - 21 June 2018.*

Wang, P., Stewart, J.P., Bozorgnia, Y., Boore, D.M. & Kishida, T. 2018. R Package for Computation of Earthquake Ground Motion Response. *PEER Report 2018/01*